

# Crossover between Thermally Assisted and Pure Quantum Tunneling in Molecular Magnet $\text{Mn}_{12}$ -Acetate

Louisa Bokacheva and Andrew D. Kent

*Department of Physics, New York University, 4 Washington Place, New York, New York 10003*

Marc A. Walters

*Department of Chemistry, New York University, 31 Washington Place, New York, New York 10003*

(June 19, 2000)

The crossover between thermally assisted and pure quantum tunneling has been studied in single crystals of high spin ( $S = 10$ ) uniaxial molecular magnet  $\text{Mn}_{12}$  using micro-Hall-effect magnetometry. Magnetic hysteresis and relaxation experiments have been used to investigate the energy levels that determine the magnetization reversal as a function of magnetic field and temperature. These experiments demonstrate that the crossover occurs in a narrow ( $\sim 0.1$  K) or broad ( $\sim 1$  K) temperature interval depending on the magnitude of the field transverse to the anisotropy axis.

PACS numbers: 75.45+j, 75.60.Ej, 75.50.Tt

High spin molecular magnets  $\text{Mn}_{12}$  and  $\text{Fe}_8$  have been actively studied as model systems for the behavior of the mesoscopic spins [1–12]. These materials can be considered as monodisperse ensembles of weakly interacting nanomagnets with net spin  $S = 10$  and strong uniaxial anisotropy. They provide a unique opportunity to study the interplay between classical thermal activation and quantum tunneling of the magnetization. Of particular interest was the observation of a regular series of steps and plateaus in magnetic hysteresis loops of  $\text{Mn}_{12}$  and  $\text{Fe}_8$  at well defined field intervals [2,3]. The steps correspond to enhanced relaxation of magnetization, and their temperature dependence suggests that both thermal activation and quantum tunneling are important to the magnetization reversal [5]. Other important results include the observation of non-exponential relaxation of magnetization [3] and quantum phase interference in  $\text{Fe}_8$  [7]. Further, EPR and inelastic neutron scattering experiments have provided important information about the magnetic energy levels of  $\text{Mn}_{12}$  and  $\text{Fe}_8$  and allowed determination of the parameters in an effective spin Hamiltonian of these clusters, relevant to understanding their macroscopic magnetic response [8–12].

Recent theoretical models of spin tunneling suggest that different types of crossovers between thermal activation over the anisotropy barrier and quantum tunneling under the barrier are possible in the large spin limit [13,14]. The crossover can occur in a narrow temperature interval with the energy at which the system crosses the anisotropy barrier shifting abruptly with temperature (denoted a first-order crossover), or the crossover can occur in a broad interval of temperature with this energy changing smoothly with temperature (second-order) [15]. The “phase diagram” for this crossover depends on the form of the spin Hamiltonian, particularly the terms important for tunneling. In finite spin systems the crossover is always smeared. Nevertheless, these scenarios are fun-

damentally different and can be distinguished experimentally. In the first case, there are competing maxima in the relaxation rate versus energy and the global maximum shifts abruptly from one energy to the other as a function of temperature. In the second-order case there is a single maximum in the relaxation rate, which shifts continuously with temperature. Recent experiments have shown that the crossover occurs in narrow temperature interval in  $\text{Mn}_{12}$  when the applied field is parallel to the easy axis of the sample [17]. In contrast, experiments on  $\text{Fe}_8$  suggest a second-order crossover [18].

In this Letter we show that in  $\text{Mn}_{12}$  the crossover indeed is one in which there are competing maxima in the relaxation rate. We show that a transverse magnetic field makes the crossover more gradual and leads to a continuous shift in the dominant energy levels with temperature (i.e., a second-order crossover). Importantly, measurements of the magnetization relaxation as a function of temperature also show evidence for a temperature independent regime below the crossover temperature.

Experimental results have been interpreted within an effective spin Hamiltonian for an individual cluster:

$$\mathcal{H} = -DS_z^2 - BS_z^4 - g_z\mu_B S_z H_z + \mathcal{H}', \quad (1)$$

where the uniaxial anisotropy parameters  $D$  and  $B$  have been determined by EPR [10] and inelastic neutron spectroscopy experiments [11] [ $D = 0.548(3)$  K,  $B = 1.17(2) \times 10^{-3}$  K, and  $g_z$  is estimated to be  $1.94(1)$ ]. Here  $\mathcal{H}'$  includes terms which do not commute with  $S_z$  and produce tunneling. These mechanisms of level mixing may be due to a transverse field (such as hyperfine fields, dipolar fields, or an external field, contributing terms such as  $H_x S_x$ ) or higher order transverse anisotropies, for example,  $C(S_+^4 + S_-^4)$ ,  $C = 2.2(4) \times 10^{-5}$  K [11], which is the lowest-order term allowed by the tetragonal symmetry of the  $\text{Mn}_{12}$  crystal. The steps in the hysteresis curves are ascribed to thermally assisted tunneling (TAT) or pure quantum tunneling (QT). According to this model,

the magnetization relaxation occurs by tunneling from magnetic sublevels ( $m = 10, 9, 8, \dots, -8, -9, -10$ ), when two levels on the opposite sides of the barrier are brought close to resonance by the magnetic field. From the unperturbed Hamiltonian (1) the longitudinal ( $z$ -axis) field at which the levels  $m_{\text{esc}}$  and  $m'$  become degenerate is:

$$H(n, m_{\text{esc}}) = nH_0\{1 + B/D[m_{\text{esc}}^2 + (m_{\text{esc}} - n)^2]\} \quad (2)$$

where  $n = m_{\text{esc}} + m'$  is the step index describing the bias field and  $H_0 = D/g_z\mu_B$  is a constant (0.42 T). The transverse anisotropy does not significantly change the resonance fields, as we have checked by direct numerical diagonalization of the Hamiltonian (1).

Note that larger magnetic field is necessary to bring lower lying sublevels into resonance. As the temperature decreases, the thermal population of the excited levels is reduced, and these states contribute less and less to the tunneling. Consequently, the steps in hysteresis curves shift to higher bias field values, and steps with larger  $n$  become observable. At low temperature, tunneling from the lowest level in the metastable well dominates, and the position and amplitude of the steps become independent of temperature, denoted the pure quantum tunneling regime (QT).

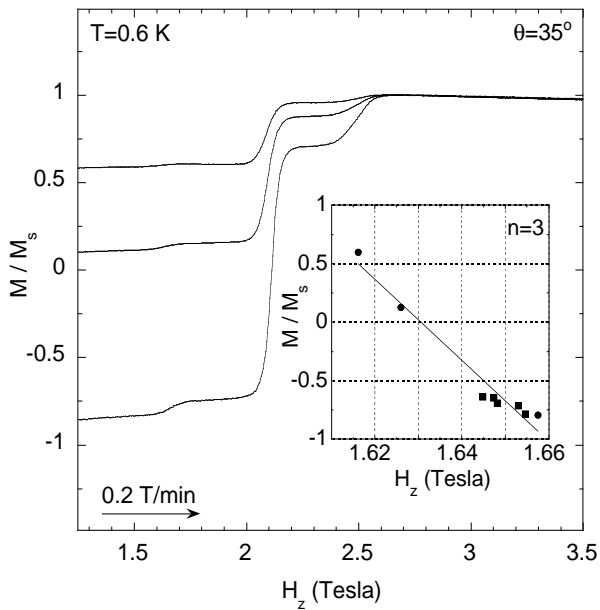


FIG. 1. Hysteresis curves of a  $\text{Mn}_{12}$  single crystal measured at  $\theta = 35^\circ$  for three different initial magnetization states:  $M_0 = 0, 0.54M_s, -M_s$ . Inset shows the change of the  $n = 3$  peak position vs magnetization at the step. Circles show data points from hysteresis measurements, squares are from field sweeps across the peak.

Our experiments have been conducted using a micro-Hall-effect magnetometer [19] in a high field helium 3 system. Single crystals of  $\text{Mn}_{12}$  in the shape of parallelepipeds  $50 \times 50 \times 200 \mu\text{m}^3$  were synthesized according to the procedure described in Ref. [20]. The crystal was encapsulated in thermally conducting grease and the temperature was measured with a calibrated carbon thermometer a few millimeters from the sample. The angle  $\theta$  between the easy axis of the crystal and the applied magnetic field was varied by rotating the sample in a superconducting solenoid. Three different orientations have been studied:  $\theta = 0^\circ, 20^\circ, \text{ and } 35^\circ$ , within an accuracy of a few degrees.

Hysteresis curves obtained for  $\theta = 35^\circ$  are shown on Fig. 1. The sample was prepared in three different initial magnetization states:  $M_0 = 0, 0.54M_s, -M_s$ , by field cooling, then the field was ramped at a constant rate (0.2 T/min) towards positive saturation. The curves show steps and plateaus, separated by a field interval of approximately 0.44 T, in agreement with previously published results. The inset of Fig. 1 shows the field position of the  $n = 3$  step versus sample magnetization at this step. The displayed data were obtained from hysteresis measurements such as those shown in Fig. 1 and from measurements in which the field was swept back and forth across the step, with the sample magnetization varying on each crossing. The peak positions are seen to depend slightly on the sample magnetization due to the average internal dipolar fields. Assuming that the peak positions are a linear function of magnetization,  $H_z = B_z - 4\pi\alpha M_z$ , an average  $\alpha$ , determined from different peaks, is approximately 0.51.

A series of isothermal hysteresis measurements have been performed in small intervals of temperature, starting with the sample initially saturated ( $M = -M_s$ ). Figure 2 shows a plot of the derivative of magnetization  $dM/dH$  versus the longitudinal applied field at different temperatures for two orientations,  $20^\circ$  and  $35^\circ$ . The positions and structure of the peaks in  $dM/dH$  show the magnetic fields at which there are maxima in the magnetization relaxation rate at a given temperature, applied field, and magnetization. The dashed lines mark the positions of the experimental maxima showing their shift with temperature. Consider the data for  $20^\circ$ , shown in Fig. 2(a). As the temperature decreases from 1.34 to 1.2 K, the maximum in  $dM/dH$  (at  $H = 1.97$  T) shifts to higher field values. At  $T = 1.24$  K, two high-field shoulders appear, which can be interpreted as the “turning on” of relaxation from energy levels closer to the bottom of the potential well. Between 1.34 and 1.17 K, amplitude in the lower field peaks is reduced, and at  $T = 1.17$  K the three peaks are of approximately equal height. However, when the temperature decreases by 0.03 K, the maximum shifts to the peak which occurs at  $H = 2.16$  T. On lowering the temperature from 1.14 to 0.94 K, the amplitude of the low-field peaks decreases, which means

that the tunneling from excited levels is “frozen out”. At  $T < 1$  K only one maximum at  $H = 2.16$  T survives, and its amplitude and position remain independent of temperature down to 0.6 K, which we associate with pure QT.

We can compare the positions of the peaks in this picture with the values of the resonant field, calculated according to Eq. (2). The high temperature regime corresponds to tunneling mostly from  $m_{\text{esc}} = 8$ , for which  $H(4, 8) = 1.97$  T. The peaks appearing at higher fields are due to tunneling from  $m_{\text{esc}} = 9$  [ $H(4, 9) = 2.06$  T] and  $m_{\text{esc}} = 10$  [ $H(4, 10) = 2.17$  T]. In the pure quantum regime the ground state,  $m_{\text{esc}} = 10$ , dominates the tunneling. The crossover from  $m_{\text{esc}} = 8$  (TAT) to  $m_{\text{esc}} = 10$  (QT) occurs over an interval of less than 0.05 K.

In contrast with this abrupt crossover, for  $\theta = 35^\circ$  the peak with the same index  $n = 4$  shifts gradually to the higher field in the range of 1.35 – 0.75 K, as shown on Fig. 2(b). Below approximately 0.75 K, the peak remains at a constant field value of 2.11 T, which indicates the transition to the quantum regime. In this case the three escape levels,  $m_{\text{esc}} = 8, 9$ , and 10 are active over comparable temperature intervals, which are marked by small steps on the dashed line.

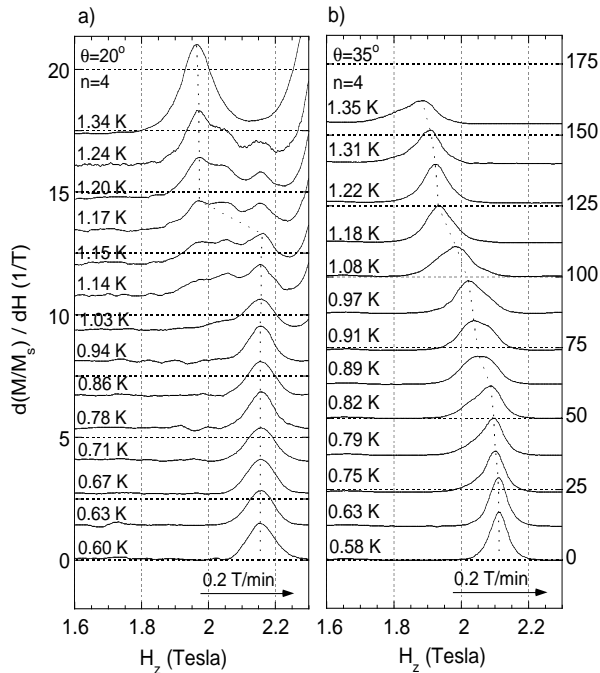


FIG. 2. Field derivative of normalized magnetization vs  $H_z$  at different temperatures for two orientations of the applied field and magnetic easy axis: a)  $\theta = 20^\circ$ , showing an abrupt crossover, and b)  $\theta = 35^\circ$ , showing a smooth crossover to QT. The curves are offset for clarity. The dashed line marks the position of the maximum in  $dM/dH$ . Note that the data on graphs a) and b) are plotted on different scales.

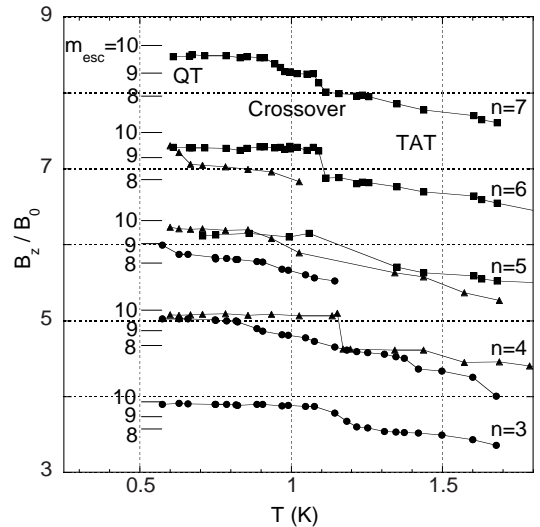


FIG. 3. Peak positions (in the units of  $B_0 = 0.42$  T) vs temperature for  $\theta = 0^\circ$  (squares),  $\theta = 20^\circ$  (triangles),  $\theta = 35^\circ$  (circles). The bars on the left hand side of the graph show the escape levels calculated using Eq. (2). The accuracy with which the peak positions can be determined is approximately the size of the symbol.

Peak position data as a function of temperature are summarized in Fig. 3, which shows the values of the longitudinal field, at which the maxima of the peaks occur, versus temperature for the three studied orientations. As mentioned above, determination of the peak positions must take into account the internal magnetic fields in the crystal. These depend on both the magnetization and the crystal shape (via the demagnetization factors). We have used the correction coefficient  $\alpha$  to determine the shift due to the magnetization of the sample:  $B_z = H_z + 4\pi\alpha M_z$ . The maximum correction is  $\Delta B_z = 8\pi\alpha M_s = 0.064$  T and is relatively small on the scale of the plot in Fig. 3. The bars on the left hand side of the figure show the escape levels calculated by using Eq. (2), with parameters from spectroscopic data [10,11]. The correspondence between these levels and the observed peak positions is remarkably good, given the approximations involved in the analysis.

By analyzing this graph, we can make following observations. First, for larger angles, and therefore higher transverse field, peaks with lower indices can be observed in the experimental time window. The lowest step observed for  $\theta = 0^\circ$  is  $n = 5$ , for  $\theta = 20^\circ$  it is  $n = 4$ , for  $\theta = 35^\circ$  it is  $n = 3$ . This is consistent with the idea that the transverse field promotes tunneling and lowers the effective anisotropy barrier. We find that there is greater amplitude in lower lying peaks as the transverse field is increased. Second, two regimes can be distinguished: the high temperature regime, where the peaks gradually shift to higher fields with decreasing temperature, and the low temperature regime, where the peak

positions are constant. We associate the first regime with the TAT and the second with pure QT. Third, the form of the crossover between these two regimes depends on the applied field. For each sample orientation, peaks with lower indices (smaller  $H_z$ ) show a more abrupt crossover between TAT and QT than peaks with higher indices (compare peaks  $n = 6$  and  $n = 7$  for  $\theta = 0^\circ$ , or  $n = 4$  and  $5$  for  $\theta = 20^\circ$ , or  $n = 3$  and  $4$  for  $\theta = 35^\circ$ ).

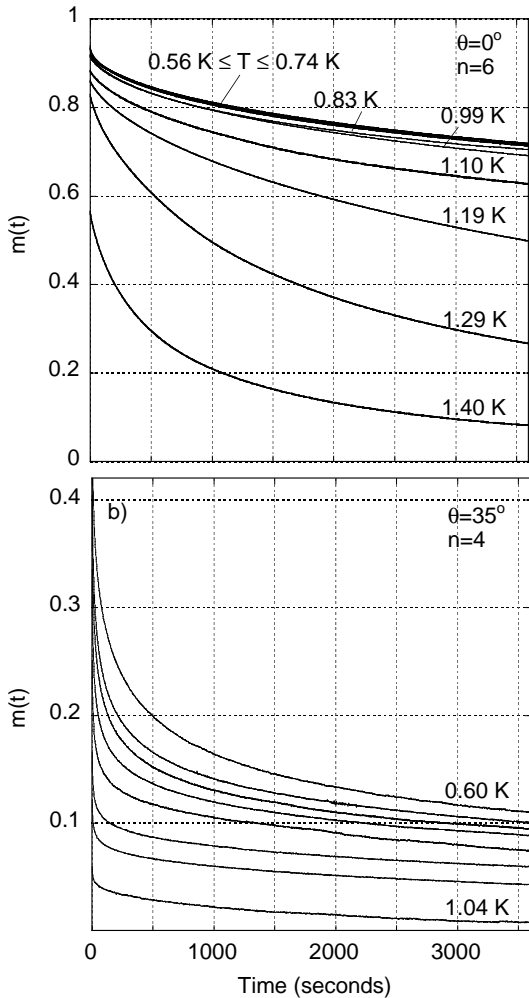


FIG. 4. Relaxation of the magnetization vs time at different temperatures for a)  $n = 6$ ,  $\theta = 0^\circ$ , showing a crossover to a quantum regime at approximately 1 K, and b)  $n = 4$ ,  $\theta = 35^\circ$ , showing no temperature independent regime.  $m(t)$  is a reduced magnetization:  $m(t) = (M_s - M(t))/2M_s$ . In a) the five curves below 0.74 K overlap (0.56 K, 0.58 K, 0.63 K, 0.68 K, 0.74 K). These curves can be fit with  $m(t) = m_0 \exp(-(t/\tau)^\beta)$ , where  $m_0 = 0.94 \pm 0.01$ ,  $\tau = (5.45 \pm 0.15) \cdot 10^4$  s,  $\beta = 0.48 \pm 0.02$ . The fit overlaps the data. In b) the unmarked curves from top to bottom correspond to  $T = 0.68$  K, 0.70 K, 0.75 K, 0.83 K, 0.91 K, 0.95 K.

The crossover from TAT to QT is also evident in magnetization relaxation measurements. In these experiments the sample was first saturated ( $M = -M_s$ ), then the field was ramped (at 0.2 T/min) to a certain value and held constant for 1 h, during which the magnetization was measured as a function of time. Figure 4 shows two sets of relaxation curves measured at  $0^\circ$  and  $35^\circ$  at the fields where peaks  $n = 6$  and  $n = 4$ , respectively, occur at the lowest temperature. For  $n = 6$ ,  $\theta = 0^\circ$  below approximately 1.1 K, the relaxation rate curves are spaced very closely, i.e., the relaxation rate almost does not change, while at higher temperature it changes significantly. This temperature corresponds to the crossover temperature seen in Fig. 3 – consistent with pure QT. In contrast, for the peak  $n = 4$ ,  $\theta = 35^\circ$ , the magnetization relaxation rate changes significantly as the temperature decreases in the entire studied range. Relaxation curves can be fit by a stretched exponential function  $m(t) = m_0 \exp(-(t/\tau)^\beta)$ , where  $\beta \approx 0.4 - 0.6$ . This form of relaxation has been observed previously in  $\text{Fe}_8$  [3] and in  $\text{Mn}_{12}$  [21], although it is not completely understood [22].

In summary, we have presented new low temperature magnetic studies of thermally assisted and pure quantum tunneling in  $\text{Mn}_{12}$ . The crossover between these two regimes was found to be either abrupt or gradual, depending on the magnitude and orientation of applied magnetic field. Higher longitudinal and transverse fields broaden the crossover, consistent with a recent model [23]. We have also shown that below the crossover temperature the magnetization relaxation becomes temperature independent. We note that the measured crossover temperature ( $\sim 1.1$  K) is significantly higher than predicted (0.6 K) [24]. This may be due to an intrinsic mechanism promoting tunneling in  $\text{Mn}_{12}$  such as a transverse anisotropy. Further studies of this crossover will lead to a better understanding of the mechanisms of relaxation in  $\text{Mn}_{12}$ .

This work was supported by NSF-INT (Grant No. 9513143) and NYU.

- 
- [1] see, E. M. Chudnovsky and J. Tejada, *Macroscopic tunneling of the magnetic moment* (Cambridge University Press, Cambridge, UK 1997), Chapter 7.
  - [2] J. R. Friedman, M. P. Sarachik, J. Tejada, and R. Ziolo, Phys. Rev. Lett. **76**, 3830 (1996); L. Thomas, F. Lioni, R. Ballou, D. Gatteschi, R. Sessoli, and B. Barbara, Nature **383**, 145 (1996).
  - [3] C. Sangregorio, T. Ohm, C. Paulsen, R. Sessoli, D. Gatteschi, Phys. Rev. Lett. **78**, 4645 (1997).

- [4] R. Sessoli, D. Gatteschi, A. Caneschi, and M. A. Novak, *Nature* **365**, 141 (1993).
- [5] M. Novak and R. Sessoli, in *Quantum Tunneling of Magnetization-QTM'94*, ed. by L. Gunther and B. Barbara (Kluwer Publishing, Dordrecht, 1995) p. 171; B. Barbara *et al.*, *JMMM* **140-144**, 1825 (1995).
- [6] J. M. Hernandez *et al.*, *Europhys. Lett.* **35**, 301 (1996).
- [7] W. Wernsdorfer and R. Sessoli, *Science* **284**, 133 (1999).
- [8] S. Hill *et al.*, *Phys. Rev. Lett.* **80**, 2453 (1998).
- [9] M. Hennion *et al.*, *Phys. Rev. B* **56**, 8819 (1997).
- [10] A. L. Barra, D. Gatteschi, and R. Sessoli, *Phys. Rev. B* **56**, 8192 (1997).
- [11] I. Mirebeau *et al.*, *Phys. Rev. Lett.* **83**, 628 (1999).
- [12] Y. Zhong *et al.*, *J. Appl. Phys.* **85**, 5636 (1999).
- [13] E. M. Chudnovsky and D. A. Garanin, *Phys. Rev. Lett.* **79**, 4469 (1997).
- [14] G.-H. Kim, *Phys. Rev. B* **59**, 11847 (1999); G.-H. Kim, *Europhys. Lett.* **51**, 216 (2000); H. J. W. Müller-Kirsten, D. K. Park, and J. M. S. Rana, *Phys. Rev. B* **60**, 6662 (1999), and references therein.
- [15] The analogy to phase transitions is a purely formal one as discussed in [13]. The first-order, second-order terminology for the escape rate crossover is originally due to Larkin and Ovchinnikov [16].
- [16] A. I. Larkin and Y. N. Ovchinnikov, *Sov. Phys. JETP* **59**, 420 (1984).
- [17] A. D. Kent *et al.*, *Europhys. Lett.* **49**, 512 (2000).
- [18] W. Wernsdorfer *et al.*, *Europhys. Lett.* **50**, 552 (2000).
- [19] A. D. Kent, S. von Molnar, S. Gider, and D. D. Awschalom, *J. Appl. Phys.* **76**, 6656 (1994).
- [20] T. Lis, *Acta Cryst. B* **36**, 2042 (1980).
- [21] L. Tomas, A. Caneschi, and B. Barbara, *Phys. Rev. Lett.* **83**, 2398 (1999).
- [22] N. V. Prokof'ev and P. C. E. Stamp, *Phys. Rev. Lett.* **80**, 5794 (1998); E. M. Chudnovsky, *Phys. Rev. Lett.* **84**, 5676 (2000); N. V. Prokof'ev and P. C. E. Stamp, *ibid.*, **84**, 5677 (2000); W. Wernsdorfer, C. Paulsen, and R. Sessoli, *ibid.*, **84**, 5678 (2000).
- [23] D. A. Garanin, X. Hidalgo, and E. M. Chudnovsky, *Phys. Rev. B* **57**, 13639 (1998).
- [24] L. Bokacheva, A. D. Kent, and M. A. Walters, *Polyhedron* (to be published).